Original Article

Increased Inflammatory Properties of Adipose Tissue Macrophages Recruited During Diet-Induced Obesity

Carey N. Lumeng,[1,2] Stephanie M. DeYoung,[1] Jennifer L. Bodzin,[1] and Alan R. Saltiel[1,3]

Although recent studies show that adipose tissue macrophages (ATMs) participate in the inflammatory changes in obesity and contribute to insulin resistance, the properties of these cells are not well understood. We hypothesized that ATMs recruited to adipose tissue during a high-fat diet have unique inflammatory properties compared with resident tissue ATMs. Using a dye (PKH26) to pulse label ATMs in vivo, we purified macrophages recruited to white adipose tissue during a high-fat diet. Comparison of gene expression in recruited and resident ATMs using real-time RT-PCR and cDNA microarrays showed that recruited ATMs overexpress genes important in macrophage migration and phagocytosis, including interleukin-6 (IL-6), inducible nitric oxide synthase (iNOS), and C-C chemokine receptor 2 (CCR2). Many of these genes were not induced in ATMs from high-fat diet–fed CCR2 knockout mice, supporting the importance of CCR2 in regulating recruitment of inflammatory ATMs during obesity. Additionally, expression of *Apoe* was decreased, whereas genes important in lipid metabolism, such as *Pparg*, *Adfp*, *Srepf1*, and *Apob48r*, were increased in the recruited macrophages. In agreement with this, ATMs from obese mice had increased lipid content compared with those from lean mice. These studies demonstrate that recruited ATMs in obese animals represent a subclass of macrophages with unique properties. *Diabetes* 56:16–23, 2007

Obesity generates a state of low-grade inflammation that is associated with the development of type 2 diabetes (1). Anti-inflammatory therapies and the disruption of genes important in proinflammatory responses, such as IκB kinase-β (IKKβ), improve insulin sensitivity in obese animals (2,3). Therefore, there is considerable interest in understanding how inflammation modifies insulin sensitivity. Factors believed to contribute to this process include increased levels of circulating cytokines, such as interleukin (IL)-6 and tumor necrosis factor-α (TNF-α), as well as tissue-specific derangements, such as hepatic inflammation and the accumulation of inflammatory macrophages in adipose tissue (4–6).

Obesity induces adipose tissue macrophage (ATM) infiltration in white adipose tissue in both humans and mice (5–7). ATM content correlates with measures of adiposity and insulin resistance (7,8). These cells are a significant source of TNF-α and IL-6 that can induce insulin resistance in adipocytes (5,6). ATMs are hypothesized to antagonize adipocyte function, participate in adipocyte death, and promote angiogenesis, but their exact functions remain unknown (9,10). Knockout mouse studies have shown that C-C chemokine receptor 2 (CCR2) and its ligand CCL2 (C-C chemokine ligand 2)/monocyte chemoattractant protein 1 (MCP-1) are required for accumulation of inflammatory macrophages in fat (11,12). CCR2 and MCP-1 knockout mice both have decreased ATM content, decreased adipose tissue inflammatory gene expression, and improved insulin sensitivity on a high-fat diet. Additionally, MCP-1 overexpression in fat tissue increases ATM content and decreases insulin responsiveness, demonstrating that ATMs are sufficient to cause insulin resistance (11,13).

Both CCR2 and MCP-1 knockout mice retain significant numbers of ATMs in their adipose tissue, despite the decrease in inflammatory gene expression. This suggests that ATMs may have diverse phenotypes, which is consistent with the current understanding of the diversity of tissue macrophages (14,15). Macrophages present in noninflamed tissues (resident macrophages) help maintain homeostasis and participate in tissue remodeling (14). In mice, these cells originate from circulating $CCR2^{-}CX3CR1^{hi}$ monocytes (16). In contrast, during an inflammatory challenge, $CCR2^{+}CX3CR1^{low}$ monocytes migrate into inflamed tissues and differentiate into macrophages, where they coordinate inflammatory responses by producing chemokines and clearing debris by phagocytosis (17). In other settings, recruited inflammatory macrophages have unique properties that include increased CD14 and TNF-α expression, decreased phagocytic ability (18,19), and unique activation states (15,20). Currently, nothing is known about ATM heterogeneity in lean and obese states, and the presence of ATMs in CCR2 and MCP-1 knockout mice suggest that a subset of ATMs function independently of CCR2.

Based on these models, we hypothesized that ATMs recruited to fat tissue during high-fat diet exposure in mice have unique properties compared with the resident ATM population, similar to what has been described in other models of inflammation. We analyzed ATMs purified using a labeling strategy that permitted isolation of these re-

From the [1]Life Sciences Institute, University of Michigan, Ann Arbor, Michigan; the [2]Department of Pediatrics and Communicable Diseases, University of Michigan Medical Center, Ann Arbor, Michigan; and the [3]Departments of Internal Medicine and Physiology, University of Michigan Medical School, Ann Arbor, Michigan.

Address correspondence and reprint requests to Alan R. Saltiel PhD, Life Sciences Institute, 210 Washtenaw Ave., Ann Arbor, MI 48109. E-mail: saltiel@lsi.umich.edu.

Received for publication 2 August 2006 and accepted in revised form 5 October 2006.

apo, apolioprotein; ATM, adipose tissue macrophage; CCR2, C-C chemokine receptor 2; DAPI, 4,6-diamidino-2-phenylindole; FACS, fluorescence-activated cell sorter; GRK3, G-protein–coupled receptor kinase 3; IL, interleukin; iNOS, inducible nitric oxide synthase; MCP-1, monocyte chemoattractant protein 1; SVF, stromal vascular fraction; TNF-α, tumor necrosis factor-α.

DOI: 10.2337/db06-1076

cruited macrophages in obese mice. Our studies identified a range of genes, including *IL-6*, inducible nitric oxide synthase (*NOS2*), and *CCR2*, that are upregulated in recruited ATMs. We also identified genes that were overexpressed in resident ATMs compared with recruited macrophages demonstrating the diverse roles ATMs assume within adipose tissue.

RESEARCH DESIGN AND METHODS

PKH26 and β-Actin monoclonal antibodies were obtained through Sigma-Aldrich (St. Louis, MO). Anti-CD68 antibody was from R&D Systems (Minneapolis, MN). Unconjugated anti-F4/80 antibodies were from Abcam (Cambridge, MA). PE-Cy5–conjugated anti-F4/80 and isotype antibodies were from eBiosciences (San Diego, CA). Alexa 488 CD11b and isotype controls were from Serotec (Raleigh, NC). CD14 antibodies were from BD Biosciences (San Jose, CA). Anti-Fgr, anti–apolioprotein (apo) E, and anti–G-protein–coupled receptor kinase 3 (GRK3) antibodies were from Santa Cruz Biotechnologies (Santa Cruz, CA).

Animals and animal care. Male C57BL/6 mice were rendered obese by feeding a high-fat diet consisting of 45% of calories from fat (Research Diets, New Brunswick, NJ) starting at 8 weeks of age for 20 weeks or the indicated times. Normal diet controls were fed a diet consisting of 4.5% of calories from fat (Labdiet, St. Louis, MO). CCR2 knockout mice on a C57BL/6 background were kindly provided by Steven Kunkel (University of Michigan). Animals were housed in a specific pathogen–free facility with a 12-h light/dark cycle and given free access to food and water. Food intake was monitored by assessing chow weight every 5 days in individually housed mice over 20 days. All animal use was in compliance with the Institute of Laboratory Animal Research Guide for Care and Use of Laboratory Animals and approved by the University Committee on Use and Care of Animals at the University of Michigan.

Stromal vascular fraction isolation. Epididymal fat pads from male C57BL/6 mice fed a normal diet or high-fat diet were excised and minced in PBS with 0.5% BSA. Tissue suspensions were centrifuged at 500*g* for 5 min to remove free erythrocytes and leukocytes. Collagenase (Sigma-Aldrich) was added to 1 mg/ml before incubation at 37°C for 20 min with shaking. The cell suspension was filtered through a 100-μm filter and spun at 300*g* for 5 min to separate floating adipocytes from the stromal vascular fraction (SVF) pellet.

For immunofluorescence and lipid staining experiments, the pellet containing SVF cells was resuspended in growth media (Dulbecco's modified Eagle's medium plus 10% heat-inactivated, endotoxin-free fetal bovine serum) and was plated on glass coverslips. For flow cytometry, the SVF pellet was incubated in 0.5 ml red blood cell lysis buffer (eBioscience) for 5 min before resuspension in sorting buffer (PBS with 0.5% fetal bovine serum, 2 mmol/l EDTA, and 25 mmol/l HEPES) at a concentration of 10^7 cells/ml. Cells were incubated with Fc Block (BD Biosciences) before staining with conjugated antibodies. After washing, cells were resuspended in sorting buffer supplemented with 4,6-diamidino-2-phenylindole (DAPI) and then analyzed using a fluorescence-activated cell sorter (FACS; FACSaria; BD Biosciences). Viable cells ($DAPI^-$) were sorted directly into RNA lysis buffer for RNA extraction. ATMs were defined as $F4/80^+CD11b^+$ cells.

Isolation of $CD11b^+$ macrophages from SVF isolates was performed by magnetic immunoaffinity isolation with anti-CD11b antibodies conjugated to magnetic beads (MACS; Miltenyi Biotec, Auburn, CA). Cells were isolated using positive selection columns before preparation of whole-cell lysates.

Immunofluorescence staining. For tissue sections, fat pads were isolated and fixed in 10% formalin overnight before cryosectioning. For cultured cells, SVF cells were plated onto glass coverslips for 2 h, and nonadherent cells were removed by washing in PBS. After 24 h, the cells were fixed in 10% formalin for 20 min. For CD68 antibody staining, cells were permeabilized with 0.5% Triton X-100 in PBS. Cells were blocked in 2% BSA in PBS and incubated with primary antibodies diluted in blocking buffer. Alexa 488–conjugated secondary antibodies were then added with or without rhodamine-conjugated phalloidin (Invitrogen, Carlsbad, CA) to label actin structures. Lipid staining was performed by incubation of fixed cells in 1 μg/ml Nile Red (Sigma-Aldrich) in PBS for 5 min. Coverslips were mounted on slides with Vectashield (Vector Laboratories, Burlingame, CA) and imaged by confocal microscopy (Olympus IX SLA; Olympus, Center Valley, PA).

PKH26 labeling of ATMs. For short-term labeling experiments, lean mice were injected via tail vein with 100 μl of saline or PKH26 (0.1 mmol/l in Diluent B) per the manufacturer's instructions. SVFs were isolated 24 h after injection and analyzed by FACS. For RT-PCR analysis, SVFs were isolated 8 weeks after injection. For microarray experiments, mice were injected with PKH26 after 8 weeks on the high-fat diet. Mice were killed 8 weeks postinjection and SVFs isolated. $F4/80^+CD11b^+PKH26^+$ and $F4/80^+CD11b^+PKH26^-$ cells were isolated by FACS and sorted into lysis buffer. Samples were isolated from three independent groups of 3–4 mice for use in microarray analysis.

Microarray and RT-PCR. RNA extraction was performed with an RNeasy kit (Qiagen, Valencia, CA). For microarray experiments, RNA quality was assessed on Agilent Bioanalyzer Picochip. RNA was amplified and cRNA prepared using Ovation Biotin labeling system (Nugen, San Carlos, CA) before hybridization to Mouse 430 2.0 arrays (Affymetrix, Santa Clara, CA). Expression values for each gene were calculated using a robust multiarray average (21). Data were filtered to remove genes without differential expression between recruited $PKH26^-$ and resident $PKH26^+$ ATM RNA samples and then fit to a linear model by the method of Smythe (22). The false discovery rate was set at an adjusted *P* value of 0.05 (23). Gene ontology was assessed using open-source databases (http://apps1.niaid.nih.gov/david/). RT reactions were performed using standard methods (Stratagene, LA Jolla, CA). cDNA were analyzed by semiquantitative PCR (30 cycles) or real-time PCR analysis using SYBR Green normalized to glyceraldehyde-3-phosphate dehydrogenase (GAPDH 7200; ABI, Foster City, CA). Semiquantitative PCR primers were: *Gapdh* forward 5′-ACCCAGAAGACTGTGGATGG-3′, *Gapdh* reverse 5′-GGAGACAACCTGGTCCTCAG-3′ (amplicon size 300 bp); *Tnfa* forward 5′-CCACATCTCCCTCCAGAAAA-3′, *Tnfa* reverse 5′-AGGGTCTGGGCCATAGAACT-3′ (amplicon size 258 bp); *Nos2* forward 5′ CAGAGGACCCAGAGACAAGC-3′, *Nos2* reverse 5′-TGCTGAAACATTTCCTGTGC-3′ (amplicon size 283 bp); *Il6* forward 5′-GTTCTCTGGGAAATCGTGGA-3′, *Il6* reverse 5′-GGAAATTCGGGGTAGGAAGGA-3′ (amplicon size 338 bp); *Ccr2* forward 5′-GGGTCATGATCCCTATGTGG-3′, *Ccr2* reverse 5′-TCCATGAGCAGTGGTTTGAA-3′ (amplicon size 215 bp); and *Cd14* forward 5′-CAAGTGGGGAACCTGTCACT-3′, *Cd14* reverse 5′-TGGCTTTTACCCACTGAACC-3′ (amplicon size 289 bp). Real-time PCR primers were: *Gapdh* forward 5′-TGAAGCAGGCATCTGAGGG-3′, *Gapdh* reverse 5′-CGAAGGTGGAAGAGTGGGAG-3′; *Adfp* forward 5′-ATTCTGAACCAGCCAACGTC-3′, *Adfp* reverse 5′-CTTATCCACCACCCCTGAGA-3′; *Apoe* forward 5′-CTGACAGGATGCCTAGCCG3′, *Apoe* reverse 5′-CGCAGGTAATCCCAGAAGC-3′; *Emb* forward 5′-TGAGGGCGATCCCACAGAT-3′, *Emb* reverse 5′-CCGTCACTGAGATATTACAGCTC-3′; *Sirpb1* forward 5′-GCTCTTGGTGAACATATCTGCC-3′, *Sirpb1* reverse 5′-GGGGTGAAGACCTTACCAGAC-3′; *Pparg* forward 5′-GGAAGACCACTCGCATTCCTT-3′, *Pparg* reverse 5′-TCGCACTTTGGTATTCTTGGAG-3′; *Fgr* forward 5′-CGGCTGAAGAACGCTATTACC-3′, *Fgr* reverse 5′-GGGCGACGAATATGGTCACTC-3′; *Fn1* forward 5′-TATAGCAGGCTACCGACTGAC-3′, *Fn1* reverse 5′-GGTCGCGGTGTACTCAGAC-3′; *Grk3* forward 5′-AGGAGGGTTTGGGGAAGTTTA-3′, *Grk3* reverse 5′-CATGATCCTCTCGTTCAAAGCC-3′; *Timp2* forward 5′-CTGGACGTTGGAGGAAAGAAG-3′, *Timp2* reverse 5′-GGTGATGCTAAGCGTGTCCC-3′; *Ccr2* forward 5′-ATCCACGGCATACTATCAACATC-3′, *Ccr2* reverse 5′-CAAGGCTCACCATCATCGTAG-3′; *Vsig* forward 5′-CCTGGGCCACCTAATAGTGC-3′, *Vsig* reverse 5′-GCCTCTCAGGGGATCATAGAT-3′; *Tnfa* forward 5′-ACGGCATGGATCTCAAAGAC-3′, *Tnfa* reverse 5′-AGATAGCAAATCGGCTGACG-3′; *Il6* forward 5′-GTTCTCTGGGAAATCGTGGA-3′, *Il6* reverse 5′-GGAAATTGGGGTAGGAAGGA-3′; *Nos2* forward 5′-CAGAGGACCCAGAGACAAGC-3′, *Nos2* reverse 5′-TGCTGAAACATTTCCTGTGC-3′; and *Cd14* forward 5′-CAAGTGGGGAACCTGTCACT-3′, *Cd14* reverse 5′-TGGCTTTTACCCACTGAACC-3′. Relative expression was assessed by comparative C_T method, correcting for amplification efficiency of the primers, and performed in triplicate.

Statistical analysis. Results are the means ± SD. Statistical analyses were conducted with unpaired Student's *t* tests, with significance set at a *P* value of <0.05.

RESULTS

Identification of ATMs via PKH26 labeling. ATMs have been identified primarily by expression of F4/80, a marker that is found on many, but not all, macrophage types (e.g., low expression in alveolar macrophages) (5,6,24). Given the heterogeneity in macrophage surface antigen expression, we sought to identify ATMs using a complementary method based on their function as phagocytic cells. To label ATMs, we injected mice intravenously with PKH26, an inert fluorescent dye that is avidly taken up by phagocytic cells in vivo and that efficiently labels tissue macrophages (18,19).

After injection with PKH26, $PKH26^+F4/80^+$ cells in the SVF were detected by FACS (Fig. 1*A*). PKH26 labeled >90% of the $F4/80^+$ cells by flow cytometry. This was confirmed in adipose tissue sections, where $PKH26^+$ cells colocalized with $CD11b^+$ cells between adipocytes and associated with vascular structures (Fig. 1*B*). Specific and efficient labeling of ATMs was further confirmed in SVF

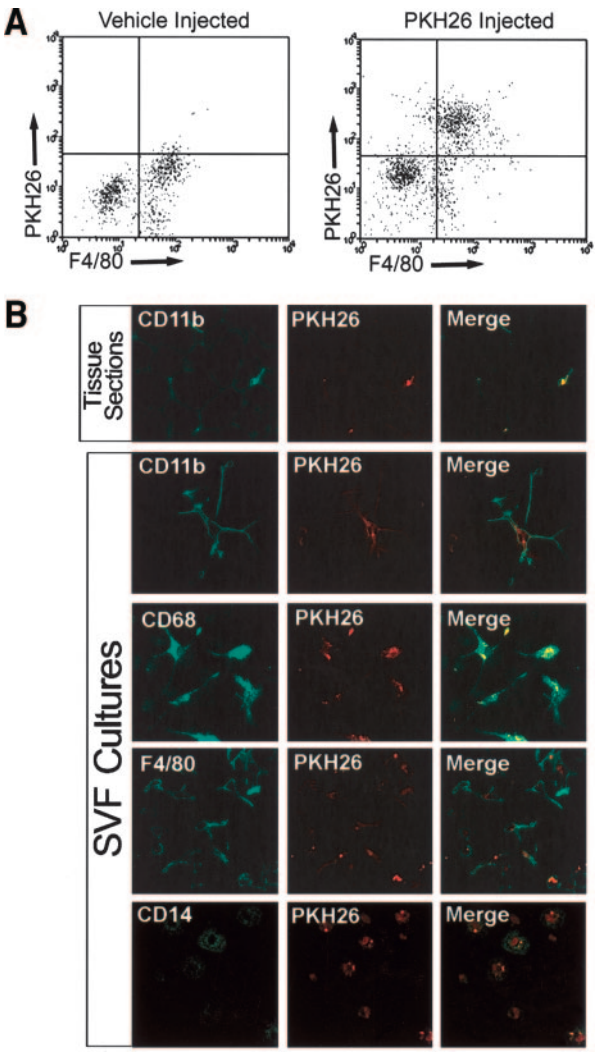

FIG. 1. Identification of ATMs based on phagocytosis of PKH26 in vivo. Male C57BL/6 mice were injected intravenously with PKH26 or PBS and analyzed by flow cytometry for PKH26 and F4/80 12 h later (*A*). Cryosections of epididymal fat (*B*, *top panel*) and SVF cells (*B*, *lower panels*) were isolated from PKH26-injected mice and stained for macrophage markers CD11b, F4/80, CD68, and CD14 before imaging by confocal microscopy.

cultures. PKH26$^+$ cells expressed CD11b, F4/80, and CD68 but showed minimal expression of CD14. ATMs extended long cellular processes and had an elongated phenotype in culture.

By immunofluorescence, variability in F4/80 expression in PKH26-labeled cells was seen with high- and low-F4/80–expressing PKH26$^+$ cells (data not shown). In contrast, CD11b labeled PKH26$^+$ cells uniformly. Therefore, subsequent studies used both CD11b and F4/80 expression to identify ATMs. PKH26 injection did not label cells lacking expression of macrophage markers F4/80 or CD11b.

Differential gene expression between resident and recruited ATMs in obese mice. Because PKH26 is retained in macrophages for prolonged periods of time (18,19,25), the efficient PKH26 labeling of ATMs in vivo allowed us to differentiate resident tissue macrophages present at the time of injection from those ATMs recruited to adipose tissue on high-fat diet exposure. Because monocytes do not take up the dye, macrophages that are recruited to adipose tissue in the days after the injection will be PKH26$^-$ (Fig. 2*A*).

To demonstrate this, mice were injected with PKH26 at 2 months of age and put on a normal diet or high-fat diet (45% kcal fat). In the high-fat diet mice, the percentage of F4/80$^+$PKH26$^-$ cells found in the SVF increased with time after injection (Fig. 2*B*). PKH26$^+$ ATMs were detectable as long as 20 weeks after injection in high-fat diet mice. In contrast, mice injected and maintained on a normal diet did not demonstrate persistence of PKH26$^+$ ATMs because they made up <5% of the ATM population at 8 weeks after injection (Fig. 2*C*). When normalized for total cell number and fat weight 8 weeks after injection, mice placed on a high-fat diet had fourfold more PKH26$^+$ ATMs compared with normal diet mice (0.25×10^6 vs. 0.063×10^6 cells/g fat). This indicates that a population of ATMs labeled by PKH26 is retained longer in high-fat diet compared with normal diet mice and suggests that ATMs in normal diet mice have a faster turnover rate than high-fat diet mice.

We hypothesized that macrophages recruited to fat tissue during high-fat diet have unique inflammatory gene expression compared with the resident macrophages. C57BL/6 male mice were injected with PKH26 and placed on high-fat diet for 8 weeks. SVF cells were then separated into an F4/80$^+$CD11b$^+$PKH26$^+$ resident ATM pool and an F4/80$^+$CD11b$^+$PKH26$^-$ recruited ATM pool (Fig. 2*D*). Gene expression in these pools was evaluated by semiquantitative RT-PCR for proinflammatory genes (Fig. 2*E*). F4/80$^+$CD11b$^+$ ATMs were also isolated by FACS from age-matched lean male mice maintained on a normal diet for comparison. Although CD14 and TNF-α were expressed at equal levels in resident and recruited ATM pools, IL-6, iNOS, and CCR2 were expressed at higher levels in the F4/80$^+$PKH26$^-$ recruited ATMs. Expression of these inflammatory genes in both recruited and resident high-fat diet ATM populations were higher than ATMs from normal diet mice. This suggests that ATMs newly recruited to adipose tissue have an increased inflammatory capacity compared with resident ATMs.

Microarray analysis of recruited and resident ATMs. These results demonstrated that for the candidate genes examined, qualitative differences exist between resident and recruited ATMs. To broadly assess gene expression differences between the two ATM subtypes, we analyzed resident and recruited ATMs using cDNA microarrays. ATMs were isolated from epididymal fat pads of three independent pools of mice injected with PKH26 and placed on high-fat diet. Because the most significant influx of macrophages into adipose tissue occurs after 8 weeks of high-fat diet (6), we designed the experiment to identify and capture the cells that accumulate in fat during the window of 8–16 weeks on a high-fat diet. Therefore, male mice were placed on a high-fat diet 8 weeks before injection and then continued on high-fat diet for 8 more weeks after injection.

Comparative analysis of gene expression between F4/80$^+$PKH26$^-$ recruited and F4/80$^+$PKH26$^+$ resident ATMs identified a total of 46 unique genes differentially expressed between the two ATM populations. Of these genes, 35 were overexpressed in recruited F4/80$^+$PKH26$^-$ ATMs (Table 1), and 11 were overexpressed in resident F4/80$^+$PKH26$^+$ ATMs (Table 2). Gene ontology analysis showed that 26% of the genes overexpressed in recruited ATMs are involved in response to stimulus or cell-cell communication (Fig. 3*A*). Genes preferentially expressed in recruited F4/80$^+$PKH26$^-$ ATMs included *Ccr2*, which agrees with studies showing that CCR2 is required for recruitment of inflammatory ATMs. Additionally, genes

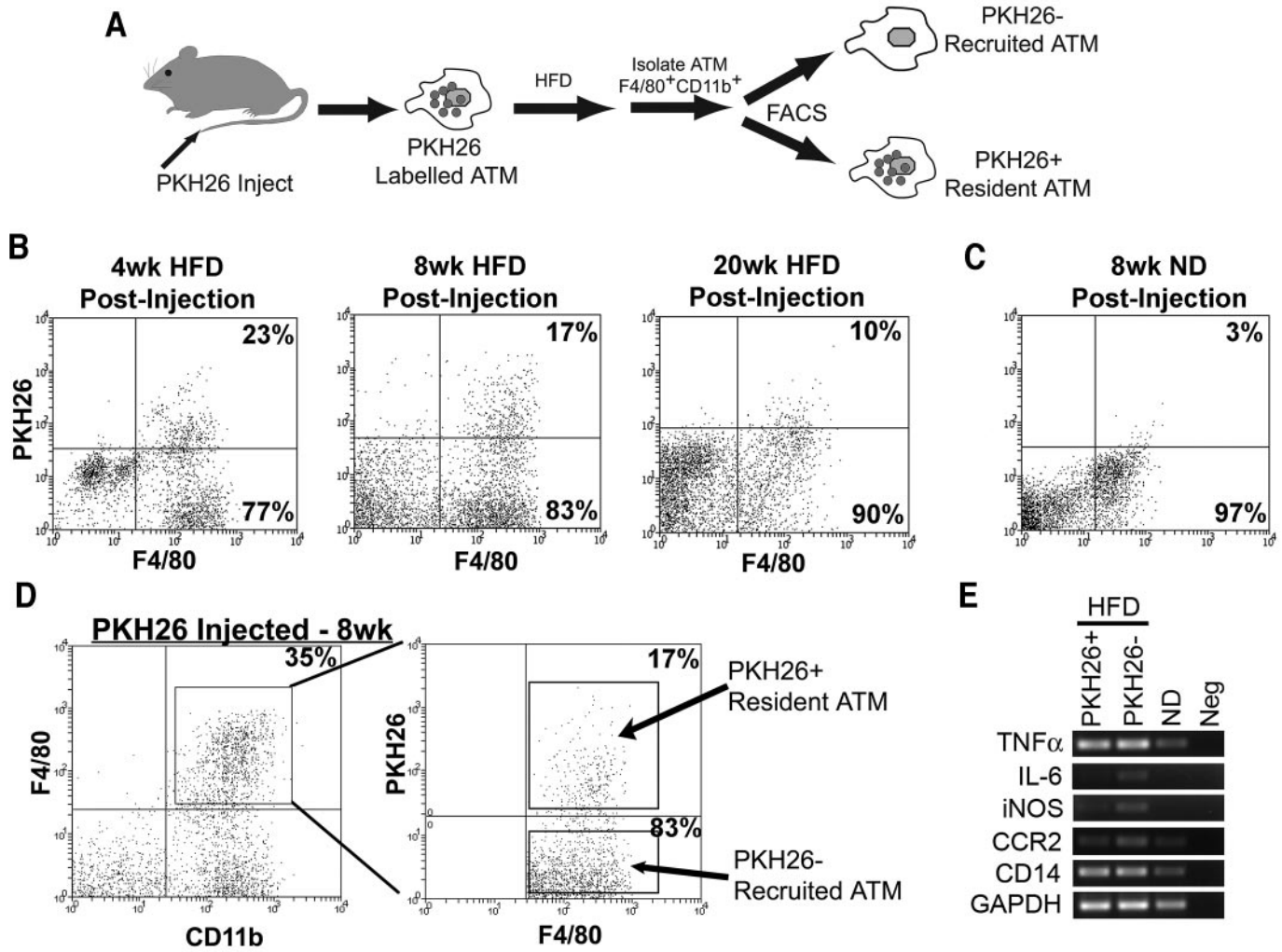

FIG. 2. Unique gene expression in ATMs recruited to adipose tissue during high-fat diet. *A*: Labeling scheme. PKH26 labeling of ATMs permits identification of PKH26$^-$ macrophages recruited to adipose tissue in the weeks after injection. FACS then separates these recruited ATMs from resident fluorescent PKH26$^+$ ATMs. *B*: SVFs from high-fat diet mice were analyzed by FACS 4, 8, and 20 weeks after injection with PKH26. The percentage of PKH26$^+$ (right upper quadrant) and PKH26$^-$ (right lower quadrant) cells within the F4/80$^+$ ATM population are shown. For comparison, mice were kept on normal diet for 8 weeks after injection (*C*) and demonstrated loss of PKH26$^+$ ATMs. For gene expression analysis, F4/80$^+$CD11b$^+$ ATMs were sorted based on PKH26 staining 8 weeks after injection (*D*), and semiquantitative RT-PCR was then performed for inflammatory genes (*E*). Similar results were obtained from two independent pools of ATMs from 2–3 mice. HFD, high-fat diet; ND, normal diet; Neg, negative; wk, week.

important in macrophage activation (signal regulatory protein β1 [*Sirpb1*] and major histocompatibility complex class II receptor [*H2-DMb1*]) and cellular adhesion and migration (embigin [*Emb*], Src kinase Fgr [*Fgr*], and fibronectin [*Fn1*]) were overexpressed in recruited ATMs. The expression differences of these genes were confirmed by real-time RT-PCR in independent unamplified RNA samples ($n = 3$) (Fig. 3*B*). Expression of all of these genes were increased in the SVF from high-fat diet mice compared with lean mice (Fig. 3*C*). Analysis of Fgr, apoE, and GRK3 by immunoblot demonstrated that these proteins were primarily expressed in ATMs compared with non-macrophage cells in the SVF (Fig. 3*D*).

Based on the current models of macrophage diversity and our microarray results (14), we hypothesized that CCR2 knockout (CCR2KO) mice would be deficient in the recruited macrophage population with high CCR2 expression, but it would retain the resident pool of ATMs (PKH26$^+$) with low CCR2 expression. Gene expression in ATMs from high-fat diet–fed CCR2KO mice was analyzed. Male CCR2KO mice did not differ in weight from C57BL/6 control mice fed a normal or high-fat diet for 16 weeks (Table 3). We did not detect significant differences in food intake between the knockout and control mice (5.95 ± 1.2 vs. 5.58 ± 0.83 g/day intake for C57/Bl6 vs. CCR2KO, P value = 0.41). A significant increase in the mass of epididymal fat pads in CCR2KO compared with control mice was observed that correlated with increased adipocyte size in the high-fat diet CCR2KO mice (data not shown) (12).

We wondered whether the genes overexpressed in the recruited ATMs might be decreased in ATMs from obese CCR2KO mice. The expression levels of these genes in ATMs from high-fat diet–fed CCR2KO mice were decreased compared with the recruited PKH26$^-$ ATMs and were expressed at levels comparable to the resident PKH26$^+$ ATM population (Fig. 3*B*). Similar results were seen for the genes overexpressed in resident ATMs, such as tissue inhibitor of metalloproteinase-2 (*Timp2*) and apoE (*Apoe*) (Fig. 3*E*). Expression levels of these genes in high-fat diet–fed CCR2KO ATMs were comparable to the resident PKH26$^+$ ATM population and were increased

TABLE 1
Genes overexpressed in recruited PKH26$^-$ ATMs compared to resident PKH26$^+$ ATMs

Gene symbol	Gene name	Fold difference	*P* value
Sirpb1	Signal-regulatory protein β1	4.25	0.026
Ear3	Eosinophil-associated, ribonuclease A family 3	3.52	0.026
Ear2	Eosinophil-associated, ribonuclease A family 2	3.38	0.017
Ccr2	Chemokine (C-C motif) receptor 2	3.2	0.017
Rasgrp1	RAS guanyl releasing protein 1	3.06	0.009
H2-DMb1	Histocompatibility 2, class II, locus Mb1	2.97	0.044
Fgr	Feline sarcoma viral (Fgr) oncogene homolog	2.71	0.044
Fn1	Fibronectin 1	2.4	0.035
Nup210	Nucleoporin 210	2.39	0.044
Tcrb-V13	T-cell receptor-β, variable 13	2.27	0.044
Ptpn22	Protein Tyr phosphatase, nonreceptor type 22	1.91	0.034
Adrbk2	Adrenergic receptor kinase, β2/GRK3	1.91	0.047
Emb	Embigin	1.87	0.017
Emr4	EGF-like module hormone receptor-like sequence 4	1.81	0.017
Mcm7	Minichromosome maintenance deficient 7	1.7	0.044
Mcm5	Minichromosome maintenance deficient 5	1.67	0.017
Cdc7	Cell division cycle 7 (*Saccharomyces cerevisiae*)	1.65	0.017
Psat1	Phosphoserine aminotransferase 1	1.54	0.044
Olfm1	Olfactomedin 1	1.53	0.026
Tigd3	Tigger transposable element derived 3	1.51	0.044
BC027057	cDNA sequence BC027057	1.50	0.017
Ezh2	Enhancer of zeste homolog 2 (*Drosophila*)	1.43	0.044
Ptger2	Prostaglandin E receptor 2 (subtype EP2)	1.29	0.05
Pold1	Polymerase (DNA directed), delta 1	1.25	0.029
Rpl17	Ribosomal protein L17	1.13	0.026
Ddx39	DEAD (Asp-Glu-Ala-Asp) box polypeptide 39	1.1	0.044
9130211I03Rik	RIKEN cDNA 9130211I03 gene	1.07	0.041
Gsto1	Glutathione S-transferase omega 1	1.04	0.05
Ptk9l	Protein tyrosine kinase 9-like (A6-related protein)	1.03	0.026
H2-DMa	Histocompatibility 2, class II, locus DMa	1.02	0.037
Myo1g	Myosin IG	1.02	0.044
Tbrg4	Transforming growth factor-β regulated gene 4	0.96	0.044
Cks1b	CDC28 protein kinase 1b	0.96	0.048
Mrps6	Mitochondrial ribosomal protein S6	0.95	0.044
Usp3	Ubiquitin specific peptidase 3	0.92	0.035

compared with the recruited PKH26$^-$ population. Combined with the morphometric data, this indicates that the qualitative changes in ATMs in the CCR2KO mice are not attributable to decreased adiposity.

High-fat diet exposure increases lipid accumulation in ATMs. ApoE (*Apoe*) gene expression was decreased in the recruited ATMs compared with resident macrophages (Fig. 3*E*). This suggested that cholesterol efflux might be impaired in recruited macrophages, similar to macrophage foam cells in atherosclerosis (26). Microarray analysis also suggested that lipid and cholesterol metabolism might be increased in recruited ATMs because expression of sterol regulatory element binding factor 1 (*Srepf1*) and apoB48 receptor (*Apob48r*) were both increased in recruited ATMs, although this did not reach full significance (P = 0.073 and 0.077, respectively).

Therefore, we examined the expression of several genes important in lipid metabolism in ATMs from normal diet and high-fat diet mice. *Apoe* was downregulated in ATMs with high-fat diet. Expression of both adipocyte differentiation–related protein (*Adfp*) and peroxisome proliferator activation receptor-γ (*Pparg*) were increased in high-fat

TABLE 2
Genes overexpressed in resident PKH26$^+$ ATMs compared to recruited PKH26$^-$ ATMs

Gene symbol	Gene name	Fold difference	*P* value
Vsig4	V-set and immunoglobulin domain containing 4	3.65	0.035
2210010L05Rik	RIKEN cDNA 2210010L05 gene	1.87	0.029
Maoa	Monoamine oxidase A	1.85	0.044
Dennd2a	DENN/MADD domain containing 2A	1.62	0.046
Timp2	Tissue inhibitor of metalloproteinase 2	1.56	0.035
Apoe	apoE	1.49	0.044
Stno	Strawberry notch homolog (*Drosophila*)	1.44	0.044
Pde2a	Phosphodiesterase 2A, cGMP-stimulated	1.42	0.041
Hrb	HIV-1 Rev binding protein	1.23	0.05
Fkbp9	FK506 binding protein 9	1.21	0.048
Dpysl3	Dihydropyrimidinase-like 3	1.01	0.044

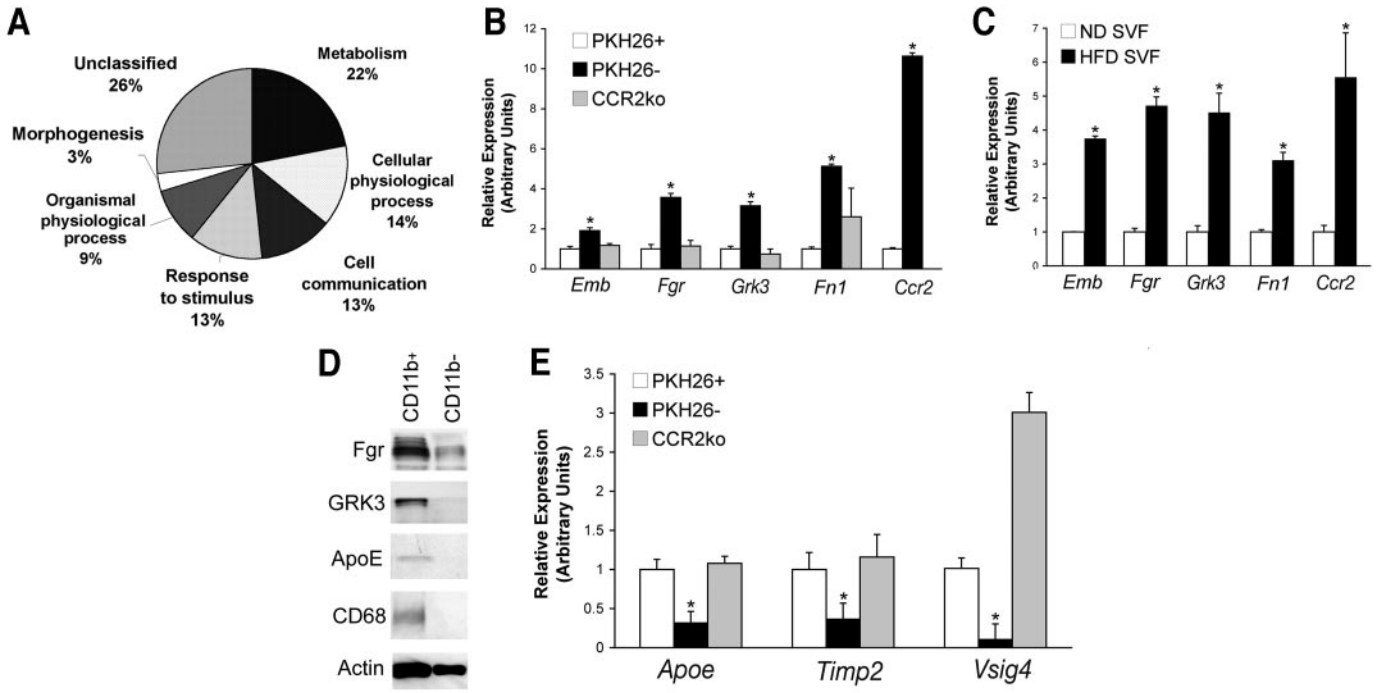

FIG. 3. Identification of genes differentially expressed between recruited and resident ATMs using microarray analysis. *A*: Ontology of genes overexpressed in recruited (PKH26$^-$) ATMs was evaluated. *B*: Differential gene expression validated by real-time RT-PCR in recruited PKH26$^-$ ATMs compared with resident PKH26$^+$ ATMs from obese mice (n = 3 pools of mice). For comparison, ATM samples from obese CCR2KO mice (*B*) and from SVF isolates from normal diet and high-fat diet mice were evaluated (*C*). Expression of Fgr, GSK-3, and apoE in ATMs was assessed by immunoblots of lysates from CD11b$^+$ ATMs compared with CD11b$^-$ nonmacrophage SVF cells (*D*). Immunoblots for CD68 demonstrate enrichment for ATMs in the CD11b$^+$ fraction. *E*: Genes identified as overexpressed in PKH26$^+$ ATMs were evaluated by real-time RT-PCR as in *B*. *$P < 0.05$. Data shows expression values as the means ± 1 SD. HFD, high-fat diet; ND, normal diet.

diet ATMs (Fig. 4*A*). To determine the functional significance of these findings, we examined the lipid content of ATMs isolated from normal diet– and high-fat diet–fed animals by Nile Red staining. Both macrophage (CD11b$^+$) and nonmacrophage (CD11b$^-$) cells in SVF cultures had Nile Red–positive vesicles; however, ATMs had more pronounced lipid accumulation, especially in obese mice (Fig. 4*B*). Lipid-rich vesicles were qualitatively larger and more abundant in ATMs from high-fat diet compared with normal diet mice (Fig. 4*C*).

DISCUSSION

We have examined the properties of ATMs in obese animals with a focus on the macrophages that are recruited to adipose tissue during high-fat diet exposure, based on the hypothesis that these cells have unique inflammatory properties. Our initial experiments examined the utility of PKH26 to label ATMs in vivo. This dye helped confirm that ATMs in mice express F4/80, CD11b, and CD68, but not CD14. Low CD14 expression appears to be a characteristic of ATMs from mice, but not from humans (27). These experiments also suggest that ATMs are the predominant phagocytic cells in the SVF.

PKH26 labeling also permitted a gross assessment of ATM turnover (rate of loss of ATMs from fat tissue). Interestingly, at 8 weeks after injection, mice on a normal diet had few PKH26$^+$ ATMs in the fat tissue, whereas those on a high-fat diet still had a significant quantity of PKH26$^+$ ATMs along with significantly more total macrophages in fat tissue compared with normal diet mice. This shows that some macrophages are retained in fat in obese mice longer than in lean animals and suggests that ATMs are lost at a greater rate in normal diet compared with high-fat diet mice. This is consistent with studies showing that CCR2$^+$ monocytes are recruited to peripheral tissues in normal states at a constant low level (28). Retention signals, such as MCP-1 and macrophage migration inhibitory factor, that are increased in obesity may serve to maintain macrophages in adipose tissue (8,29). Further studies are required to confirm this hypothesis, using other methods such as bone marrow transplantation.

Stratification of ATMs based on PKH26 labeling allowed us to purify ATMs that are recruited to white fat during high-fat diet exposure (PKH26$^-$). This pulse labeling technique has been used in other inflammatory settings to examine the properties of recruited tissue macrophages. Recruited ATMs had increased expression of *Ccr2*, *Il6*, and *Nos2*, genes that have been previously shown to contribute to inflammation in adipose tissue (5,6,12).

TABLE 3
Body weights and epididymal fat pad weights of mice used in gene expression analyses

	Body weight (g)	Epididymal fat pad weight (g)
C57Bl/6 normal diet	28.98 ± 1.5	0.30 ± 0.10
C57Bl/6 high-fat diet	44.93 ± 4.2*	1.85 ± 0.28†
CCR2KO normal diet	29.13 ± 0.81	0.49 ± 0.06‡
CCR2KO high-fat diet	49.55 ± 5.3§	2.70 ± 0.58‖

n = 5–6 mice per group. *$P < 0.001$ vs. C57 normal diet; †$P < 0.001$ vs. C57 normal diet; ‡$P < 0.05$ vs. C57 normal diet; §$P < 0.001$ vs. CCR2KO normal diet; ‖$P < 0.001$ vs. CCR2KO normal diet, <0.05 vs. C57.

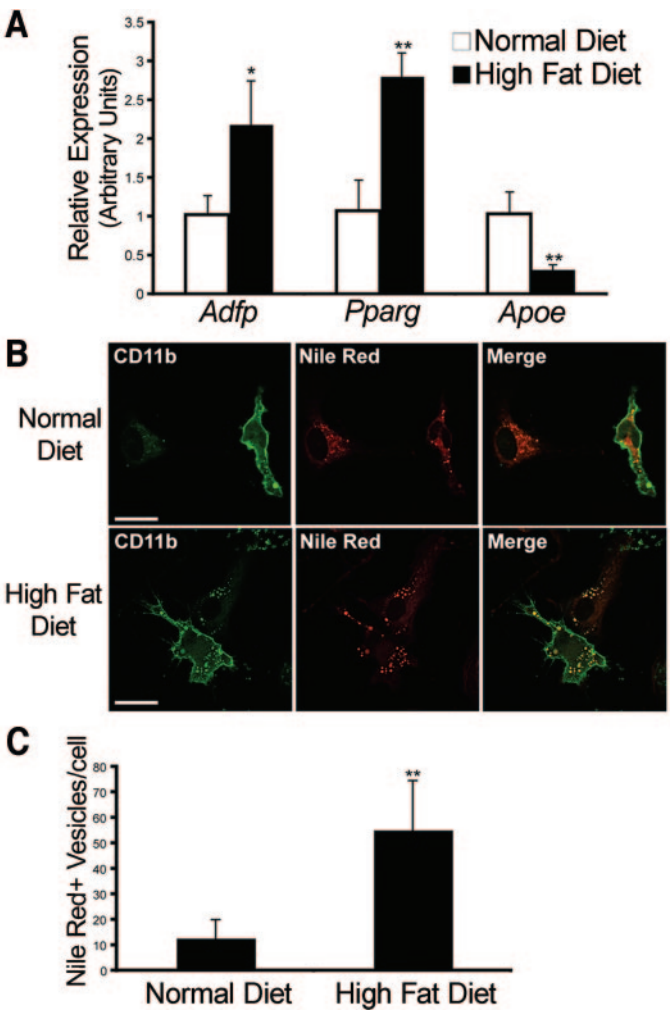

FIG. 4. Lipid accumulation in ATMs with high-fat diet. *A*: Expression of lipid-responsive genes assessed in ATMs isolated from normal diet– and high-fat diet–fed male C57BL/6 mice. Relative expression is the means ± 1 SD. *B*: Lipid accumulation assessed in ATMs by staining SVF cultures from normal diet and high-fat diet mice with CD11b and Nile Red to identify lipid droplets. *C*: Lipid accumulation quantitated by microscopy. *N* >30 cells for each. Data are the means ± 1 SD. **P* < 0.05; ***P* < 0.005.

These observations support the importance of the CCR2/MCP-1 axis in recruiting ATMs during high-fat diet.

To better understand these cell types, we used microarray analysis to examine differential gene expression between resident and recruited ATMs in obese animals. The validity of this approach was highlighted by the detection of increased CCR2 expression in PKH26$^-$ recruited ATMs. We identified a number of other genes involved in macrophage inflammatory responses, migration, and phagocytosis that are upregulated in recruited PKH26$^-$ ATMs.

Embigin, fibronectin, and the Src kinase Fgr are important in cell migration and were all increased in recruited ATMs. The importance of cell adhesion in ATM function was supported by the long processes seen in cultured ATMs from obese mice. This supports observations that macrophage-adipocyte cell contact activates macrophages and influences adipocyte insulin sensitivity (30). Additionally, recruited ATMs had increased expression of major histocompatibility complex class II receptors, suggesting that these macrophages have increased antigen-presenting properties.

Based on a panel of genes identified in microarrays, ATMs from obese CCR2KO mice have characteristics similar to the resident population of ATMs and differ from the recruited population of ATMs. This is consistent with the model that resident ATMs arrive in fat via CCR2-independent signals and have decreased inflammatory properties. How such cells get targeted to adipose tissue is unknown. Overall, these observations demonstrate a diversity in ATMs from obese mice that has not been previously appreciated, and they imply that some macrophages in fat tissue may have decreased inflammatory properties.

Our analysis of diet-induced obesity in CCR2KO mice differs from other reports on this model (12,31). Similar to Chen et al. (31), we observed equivalent weight gain on a high-fat diet in CCR2KO mice and controls. This differs from the data of Weisberg et al. (12), who observed less weight gain in CCR2KO mice based on decreased food intake. These discrepancies may be due to different diet compositions between studies (60% fat for Weisberg et al. vs. 45% fat in this study), differences in animal care, or differences in food intake analysis. Similar to Weisberg et al. (12), we observed increased adipocyte size and protection from hepatic steatosis in high-fat diet–fed CCR2KO mice. However, we observed increased weight of epididymal fat pads in normal diet– and high-fat diet–fed CCR2KO mice compared with controls, whereas Weisberg et al. did not note differences in total fat mass by dual-energy X-ray absorptiometry analysis. This difference may be attributable either to the different feeding protocols used (Weisberg et al. fed 60% fat for 24 weeks) or to the different methodologies used to assess fat composition.

We did not note differences in TNF-α expression between the resident and recruited ATMs from high-fat diet mice in both RT-PCR and microarray analysis, and we observed that both types express more TNF-α than ATMs from lean animals. This suggests that obesity generates signals that may activate all macrophages similarly in fat, despite the qualitative differences between subtypes of ATMs. Although the role of TNF-α in adipose tissue function is well known, these findings suggest that other macrophage characteristics should be examined further, including cell adhesion and migratory properties.

Our microarray analysis failed to identify significant differences in cytokine gene expression between the recruited and resident ATM populations, which differed from our initial analysis of these cytokines. This may be attributable to loss of sensitivity with the RNA amplification step required for the microarray hybridization. Alternatively, the experimental design used for the microarray analysis may examine slightly different ATM populations. Nevertheless, this analysis provides evidence of qualitative differences in ATM subpopulations that is a starting point for future investigations.

High-fat diet appears to increase ATM expression of genes important in lipid metabolism, such as *Adfp*, *Pparg*, *Srebf1*, and *Apob48r*. Increased *Adfp* expression supports studies that show increased adipocyte differentiation–related protein in ATMs in crown-like structures (9). Increases in *Apob48r* and *Srebf1* are consistent with the increased lipid uptake seen in high-fat diet ATMs. These observations are similar to what has been seen with foam cells in atherosclerosis and suggest that similar mechanisms may relate the two processes.

It is important to point out that these observations were made in murine models of diet-induced obesity and that the changes identified here may not be recapitulated in

humans. Mouse and human macrophages differ with respect to activation profiles (15). In particular, iNOS activity in macrophage populations differs between murine and human models of inflammation (32,33). However for many inflammatory markers, ATMs from obese humans and mice have been shown to be similar (5–7). Therefore, mice remain a useful model for examining ATM biology to generate new hypotheses to be confirmed in humans. Future studies will focus on defining the importance of the identified genes on ATM function and the development of type 2 diabetes. They will enable us to better understand the range of function of these unique cells and to investigate how their diversity may be used to control inflammation in adipose tissue.

ACKNOWLEDGMENTS

Research was supported by a training grant from the National Institutes of Health to the Department of Pediatrics and Communicable Diseases (T32HD007513), a grant to the Michigan Diabetes Research Training Center (P60DK20572), and a grant from the National Institutes of Health (R01DK60591) to A.R.S.

We thank the University of Michigan Flow Cytometry Core for their assistance with FACS analysis and the University of Michigan Microarray Core for microarray hybridization and data analysis. We thank the Michigan Diabetes Research Training Center at the University of Michigan for subsidizing microarray analysis costs. We thank Jiandie Lin for his assistance with real-time PCR.

REFERENCES

1. Shoelson SE, Lee J, Goldfine AB: Inflammation and insulin resistance. *J Clin Invest* 116:1793–1801, 2006
2. Kim JK, Kim YJ, Fillmore JJ, Chen Y, Moore I, Lee J, Yuan M, Li ZW, Karin M, Perret P, Shoelson SE, Shulman GI: Prevention of fat-induced insulin resistance by salicylate. *J Clin Invest* 108:437–446, 2001
3. Yuan M, Konstantopoulos N, Lee J, Hansen L, Li ZW, Karin M, Shoelson SE: Reversal of obesity- and diet-induced insulin resistance with salicylates or targeted disruption of Ikkbeta. *Science* 293:1673–1677, 2001
4. Cai D, Yuan M, Frantz DF, Melendez PA, Hansen L, Lee J, Shoelson SE: Local and systemic insulin resistance resulting from hepatic activation of IKK-beta and NF-kappaB. *Nat Med* 11:183–190, 2005
5. Weisberg SP, McCann D, Desai M, Rosenbaum M, Leibel RL, Ferrante AW Jr: Obesity is associated with macrophage accumulation in adipose tissue. *J Clin Invest* 112:1796–1808, 2003
6. Xu H, Barnes GT, Yang Q, Tan G, Yang D, Chou CJ, Sole J, Nichols A, Ross JS, Tartaglia LA, Chen H: Chronic inflammation in fat plays a crucial role in the development of obesity-related insulin resistance. *J Clin Invest* 112:1821–1830, 2003
7. Cancello R, Henegar C, Viguerie N, Taleb S, Poitou C, Rouault C, Coupaye M, Pelloux V, Hugol D, Bouillot JL, Bouloumie A, Barbatelli G, Cinti S, Svensson PA, Barsh GS, Zucker JD, Basdevant A, Langin D, Clement K: Reduction of macrophage infiltration and chemoattractant gene expression changes in white adipose tissue of morbidly obese subjects after surgery-induced weight loss. *Diabetes* 54:2277–2286, 2005
8. Di Gregorio GB, Yao-Borengasser A, Rasouli N, Varma V, Lu T, Miles LM, Ranganathan G, Peterson CA, McGehee RE, Kern PA: Expression of CD68 and macrophage chemoattractant protein-1 genes in human adipose and muscle tissues: association with cytokine expression, insulin resistance, and reduction by pioglitazone. *Diabetes* 54:2305–2313, 2005
9. Cinti S, Mitchell G, Barbatelli G, Murano I, Ceresi E, Faloia E, Wang S, Fortier M, Greenberg AS, Obin MS: Adipocyte death defines macrophage localization and function in adipose tissue of obese mice and humans. *J Lipid Res* 46:2347–2355, 2005
10. Neels JG, Olefsky JM: Inflamed fat: what starts the fire? *J Clin Invest* 116:33–35, 2006
11. Kanda H, Tateya S, Tamori Y, Kotani K, Hiasa K, Kitazawa R, Kitazawa S, Miyachi H, Maeda S, Egashira K, Kasuga M: MCP-1 contributes to macrophage infiltration into adipose tissue, insulin resistance, and hepatic steatosis in obesity. *J Clin Invest* 116:1494–1505, 2006
12. Weisberg SP, Hunter D, Huber R, Lemieux J, Slaymaker S, Vaddi K, Charo I, Leibel RL, Ferrante AW: CCR2 modulates inflammatory and metabolic effects of high-fat feeding. *J Clin Invest* 116:115–124, 2005
13. Kamei N, Tobe K, Suzuki R, Ohsugi M, Watanabe T, Kubota N, Ohtsuka-Kowatari N, Kumagai K, Sakamoto K, Kobayashi M, Yamauchi T, Ueki K, Oishi Y, Nishimura S, Manabe I, Hashimoto H, Ohnishi Y, Ogata H, Tokuyama K, Tsunoda M, Ide T, Murakami K, Nagai R, Kadowaki T: Overexpression of MCP-1 in adipose tissues causes macrophage recruitment and insulin resistance. *J Biol Chem* 281:26602–26614, 2006
14. Gordon S, Taylor PR: Monocyte and macrophage heterogeneity. *Nat Rev Immunol* 5:953–964, 2005
15. Mantovani A, Sica A, Sozzani S, Allavena P, Vecchi A, Locati M: The chemokine system in diverse forms of macrophage activation and polarization. *Trends Immunol* 25:677–686, 2004
16. Geissmann F, Jung S, Littman DR: Blood monocytes consist of two principal subsets with distinct migratory properties. *Immunity* 19:71–82, 2003
17. Hume DA: The mononuclear phagocyte system. *Curr Opin Immunol* 18:49–53, 2006
18. Jennings JH, Linderman DJ, Hu B, Sonstein J, Curtis JL: Monocytes recruited to the lungs of mice during immune inflammation ingest apoptotic cells poorly. *Am J Respir Cell Mol Biol* 32:108–117, 2005
19. Maus U, Herold S, Muth H, Maus R, Ermert L, Ermert M, Weissmann N, Rosseau S, Seeger W, Grimminger F, Lohmeyer J: Monocytes recruited into the alveolar air space of mice show a monocytic phenotype but upregulate CD14. *Am J Physiol Lung Cell Mol Physiol* 280:L58–L68, 2001
20. Gordon S: Alternative activation of macrophages. *Nat Rev Immunol* 3:23–35, 2003
21. Irizarry RA, Hobbs B, Collin F, Beazer-Barclay YD, Antonellis KJ, Scherf U, Speed TP: Exploration, normalization, and summaries of high density oligonucleotide array probe level data. *Biostatistics* 4:249–264, 2003
22. Smyth GK: Linear models and empirical bayes methods for assessing differential expression in microarray experiments. *Stat Appl Genet Mol Biol* 3:Article3, 2004
23. Benjamini Y, Hochberg Y: Controlling the false discovery rate: a practical and powerful approach to multiple testing. *J Royal Statistical Soc B* 57:289–300, 1995
24. Vermaelen K, Pauwels R: Accurate and simple discrimination of mouse pulmonary dendritic cell and macrophage populations by flow cytometry: methodology and new insights. *Cytometry A* 61:170–177, 2004
25. Horan PK, Melnicoff MJ, Jensen BD, Slezak SE: Fluorescent cell labeling for in vivo and in vitro cell tracking. *Methods Cell Biol* 33:469–490, 1990
26. Greenow K, Pearce NJ, Ramji DP: The key role of apolipoprotein E in atherosclerosis. *J Mol Med* 83:329–342, 2005
27. Prunet-Marcassus B, Cousin B, Caton D, Andre M, Penicaud L, Casteilla L: From heterogeneity to plasticity in adipose tissues: site-specific differences. *Exp Cell Res* 312:727–736, 2006
28. Xu H, Manivannan A, Dawson R, Crane IJ, Mack M, Sharp P, Liversidge J: Differentiation to the CCR2+ inflammatory phenotype in vivo is a constitutive, time-limited property of blood monocytes and is independent of local inflammatory mediators. *J Immunol* 175:6915–6923, 2005
29. Skurk T, Herder C, Kraft I, Muller-Scholze S, Hauner H, Kolb H: Production and release of macrophage migration inhibitory factor from human adipocytes. *Endocrinology* 146:1006–1011, 2005
30. Lumeng CN, Deyoung SM, Saltiel AR: Macrophages block insulin action in adipocytes by altering expression of signaling and glucose transport proteins. *Am J Physiol Endocrinol Metab*. In press
31. Chen A, Mumick S, Zhang C, Lamb J, Dai H, Weingarth D, Mudgett J, Chen H, MacNeil DJ, Reitman ML, Qian S: Diet induction of monocyte chemoattractant protein-1 and its impact on obesity. *Obes Res* 13:1311–1320, 2005
32. Schneemann M, Schoedon G: Species differences in macrophage NO production are important (Comment). *Nat Immunol* 3:102, 2002
33. Zhang X, Laubach VE, Alley EW, Edwards KA, Sherman PA, Russell SW, Murphy WJ: Transcriptional basis for hyporesponsiveness of the human inducible nitric oxide synthase gene to lipopolysaccharide/interferon-gamma. *J Leukoc Biol* 59:575–585, 1996